Fluorescence, Circular Dichroism, Light Scattering, and Microscopic Characterization of Vesicles of Sodium Salts of Three *N*-Acyl Peptides

Dibyendu Khatua and Joykrishna Dey*,†

Department of Chemistry, Indian Institute of Technology, Kharagpur −721 302, India

Received: August 13, 2006; In Final Form: November 7, 2006

Aggregation behavior of three *N*-acyl peptide surfactants, sodium *N*-(4-n-dodecyloxybenzoyl)-L-alyl-L-valinate (SDBAV), L-valyl-L-alaninate (SDBVA), and L-valyl-L-valinate (SDBVV), were investigated. The amphiphiles have very low critical aggregation concentration (cac). Fluorescence anisotropy studies using 1,6-diphenyl-1,3,5-hexatriene (DPH) as a fluorescent probe indicated formation of bilayer aggregates in dilute solution. Transmission electron micrographs showed the existence of large vesicles in dilute solution. Circular dichroism spectra suggested formation of helical aggregates. The vesicle formation was found to be more favored at neutral pH. Dynamic light scattering was used to measure hydrodynamic radius of the vesicles. The microviscosity of the vesicles formed by the amphiphiles was determined by use of fluorescence anisotropy and the lifetime of the DPH probe. The vesicles formed by the surfactants are stable at temperatures above body temperature and for a long period of time. Fluorescence probe studies, however, indicated transformation of vesicles to rod-like micelles at surfactant concentrations much higher than the cac value. Addition of sodium chloride also transformed the vesicles to rod-like micelles.

1. Introduction

It is well-known that *N*-acyl amino acid surfactants (NAAS) produce a range of bilayer structures including spherical vesicles, tubules, ribbons, etc. in aqueous solutions above their critical aggregation concentration.[1−10] Recent work in our laboratory has shown that hydrogen-bonding interactions (HBI) between amide groups at the surfactant tail also promote formation of bilayer structures by sodium 11-acrylamidoundecanoate in water.[11] More recently, one of us has investigated the aggregation behavior of sodium *N*-(4-n-dodecyloxybenzoyl)-L-valinate (SDBV) in aqueous solutions.[12] This surfactant was found to form vesicles spontaneously above a very low critical vesicle concentration (cvc). We have also shown that SDBV produces chiral helical aggregates in water at a higher concentration. Because amide hydrogen bonding at the surfactant head group has been proposed to be responsible for the formation of helical aggregates, we wanted to investigate if introduction of another amide group enhances chirality of the helical aggregates. Warner and co-workers have reported aggregation behavior of the sodium salts of a series of *N*-acyl derivatives of dipeptides in aqueous solutions.[13] These authors have found that the micelles formed by these surfactants have large aggregation numbers as a result of strong HBI between amide groups of adjacent molecules in the self-assemblies. In the present work, we have chosen three surfactants whose head groups consist of a peptide bond. We have synthesized sodium *N*-(4-n-dodecyloxybenzoyl)-L-alayl-L-valinate (SDBAV), sodium *N*-(4-n-dodecyloxybenzoyl)-L-valyl-L-alaninate (SDBVA), and sodium *N*-(4-n-dodecyloxybenzoyl)-L-valyl-L-valinate (SDBVV) (see Chart 1 for structures) and studied their self-assembly properties in aqueous solutions. The new surfactants have been designed in light of their potential use as chiral selectors in micellar electrokinetic chromatography. The focus of this study is to investigate the effect of the order of the amino acid residues in the dipeptide head group on surface and aggregation behavior of the surfactants. Various techniques such as surface tension, fluorescence probe, dynamic light scattering (DLS), and transmission electron microscopy (TEM) have been used to characterize the self-assemblies formed by the surfactants. The circular dichroism (CD) spectra were recorded to examine chiral aggregate formation.

CHART 1: Chemical structures of SDBVA, SDBAV, and SDBVV

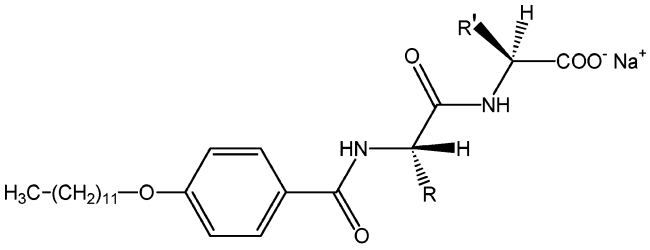

$R = CH_3,\ R' = CH(CH_3)_2$ (SDBAV)

$R = CH(CH_3)_2,\ R' = CH_3$ (SDBVA)

$R = CH(CH_3)_2,\ R' = CH(CH_3)_2$ (SDBVV)

2. Experimental Section

2.1. Materials. All amino acids and bromododecane were from SRL and were used directly from the bottles. Potassium carbonate and sodium chloride were obtained locally and used directly. Pyrene, *N*-phenyl-1-naphthylamine (NPN), and 1,6-diphenyl-1,3,5-hexatriene (DPH) were purchased from Aldrich

* Corresponding author. Telephone: +91-3222-283308. Fax: +91-3222-255303. E-mail: joydey@chem.iitkgp.ernet.in.

† Current affiliation: Biophysical-Analytical Laboratory, Department of Chemistry, Indian Institute of Technology, Kharagpur −721 302, India.

10.1021/jp065225w CCC: $37.00
Published on Web 12/13/2006

and used after recrystallization from an acetone−ethanol mixture. Purity of the probes was tested by the fluorescence emission and excitation spectra. Aqueous solutions were prepared using doubly distilled water. All solvents were distilled and dried before use. The synthesis and chemical identification of the *N*-acyl peptides have been described in the Supporting Information.

2.2. General Instruments. ^{1}H−NMR spectra were recorded on a Bruker SEM 200 instrument in $CDCl_3$ solvent. The FT−IR spectra were measured with a Thermo Nicolet Nexus 870 spectrometer using KBr pellets. The UV−vis spectra were recorded on a Shimadzu (model 1601) spectrophotometer. The surface tension measurements were performed with a Torsion Balance (S.D. Hurdson & Co., Kolkata) using the Du Nüoy ring detachment method. The specific rotations were measured with a Jasco P-1020 digital polarimeter. The melting point was determined by use of an Instind (Kolkata) melting point apparatus in open capillaries. A Thermo Orion model 710A+ digital pH meter was used to measure the pH of the solutions. Temperature controlled measurements were carried out by use of a Thermo Neslab RTE −7 circulating bath.

2.3. Steady-State Fluorescence Mesurements. Steady-state fluorescence spectra were recorded with a SPEX Fluorolog model FL-2 spectrofluorometer. Saturated aqueous solutions of NPN and pyrene were used for sample preparation. The samples containing NPN and pyrene were excited at 350 and 335 nm, respectively, using both an excitation and emission bandpass of 1 nm. All spectra were blank subtracted.

A Perkin-Elmer LS-55 luminescence spectrometer equipped with filter polarizers that uses the L-format configuration using a 1 cm^2 quartz cuvette was used for fluorescence depolarization measurements. Because DPH is insoluble in water, a 1.0 mM stock solution of the probe in a 20% (v/v) methanol−water mixture was prepared. The final concentration of the probe was adjusted to 1.0 μM by addition of an appropriate amount of the stock solution. The anisotropy measurements were carried out in the temperature range 20−60 °C and pH 9.1. The samples containing DPH were excited at 350 nm, and the emission intensity was followed at 450 nm using excitation slit with a 2.5 nm bandpass. The emission bandpass varied between 2.5 and 7.5 nm. A 430 nm cutoff filter was placed in the emission beam to eliminate the effects of scattered radiation. A 10 s integration time was used for data collection. The *r*-value was calculated employing the equation

$$r = (I_{VV} - GI_{VH})/(I_{VV} + 2GI_{VH}) \quad (1)$$

where I_{VV} and I_{VH} are the fluorescence intensities polarized parallel and perpendicular to the excitation light and G is the instrumental correction factor ($G = I_{HV}/I_{HH}$). An average of six measurements was always recorded. The fluorescence measurements were done at pH 9.1 and at 30 °C.

2.4. Dynamic Light Scattering. The dynamic light scattering (DLS) measurements were performed using a Malvern 4800 Autosizer employing a 7132 correlator. The light source was an argon ion laser of wavelength 514.5 nm with a maximum output power of 2 W. The scattering intensity was measured at different angles (θ) in the range $45° < \theta < 150°$. Surfactant solutions were prepared in double distilled water. The solution was filtered through a Millipore Millex syringe filter (0.22 μm) directly into the scattering cell. Prior to the measurements, the scattering cell was rinsed several times with the filtered solution. The DLS measurements started 5−10 min after the sample solutions were placed in the DLS optical system to allow the sample to equilibrate at the bath temperature. For all light scattering measurements, the temperature was 30 ± 0.5 °C. The average decay rate (Γ) of the electric field autocorrelation function, $g^1(\tau)$, was estimated using the cumulants method. The apparent diffusion coefficient (D) of the vesicles was obtained from the relation $\Gamma = Dq^2$ (q being the magnitude of the scattering vector, given by $q = [4\pi n \sin(\theta/2)]/\lambda$; n and λ are the refractive index of the solvent and the wavelength of the laser light, respectively). The corresponding hydrodynamic diameter of the particles was calculated using the Stokes−Einstein relationship.

TABLE 1: Physicochemical Properties of SDBAV, SDBVA, and SDBVV in Water (pH 9.1) at 30 °C

properties	SDBAV	SDBVA	SDBVV
cac (mM)	0.02	0.02	0.04
	0.02[a]	0.03[a]	0.04[a]
r	0.155	0.178	0.190
I_1/I_3	1.43	1.19	1.15
η_m (mPa s)	80.6	89.3	110.9, 42.7[b]
R_h (nm)	57.0, 44.0[c]	116	81.0, 65.0[d]
pK_a	7.2	6.7	6.9
T_c (°C)	46.5	34.4	40

[a] Obtained from fluorescence measurement with NPN probe. [b] Data correspond to 1.0 mM surfactant. [c,d] Measured at concentrations 0.2 and 1.0 mM, respectively.

2.5. Transmission Electron Microscopy (TEM). The TEM measurements were performed using a 0.25 mM (for SDBVA and SDBAV) or 1 mM (for SDBVV) solution of the amphiphiles after equilibration for 2−3 h. A carbon-coated copper grid was immersed in a drop of aqueous solution of the amphiphile for 1 min, blotted with filter paper, air-dried, and then negatively stained with freshly prepared 2.0% aqueous uranyl acetate. The specimens were kept in desiccators until use. The specimens were examined on a Phillips CM 200 electron microscope operating at an accelerating voltage of 200 kV at room temperature.

3. Results and Discussion

3.1. Critical Aggregation Concentration. Surface tensiometry (ST) is the most commonly used method for determination of critical aggregation concentration (cac) of surfactants. The surface tension (γ) was measured in water as a function of increasing surfactant concentration. The pH of water was adjusted to 9.1 with dilute NaOH solution to make sure that the amphiphiles remain fully ionized. The concentration corresponding to the breakpoint in the plot of γ vs log[surfactant] was taken as the cac value. The data are listed in Table 1. The plots have been shown in Figure S1 in the Supporting Information. Normally, cac values obtained by the ST method are considered most accurate. However, the cac values obtained by ST measurements were further verified by a fluorescence probe method using NPN as a probe molecule. It is reported that there is a huge increase in fluorescence emission intensity accompanied by a large blue shift ($\Delta\lambda = \lambda_{water} - \lambda_{surfactant}$) of the emission maximum of NPN relative to that in pure water upon solubilization in the hydrophobic environment of surfactant aggregates.[14] Therefore, fluorescence spectra of NPN were measured in the presence of different concentrations of the amphiphiles. The plots of relative fluorescence intensity (F/F_o) versus [surfactant] (Figure S2) are available in the Supporting Information. The cac values obtained from the inflection point (as indicated in the plot) of the respective plots are included in Table 1. It can be observed that with the exception of SDBVA the cac values of the amphiphiles thus obtained are equal to the corresponding value obtained by the ST method. The large

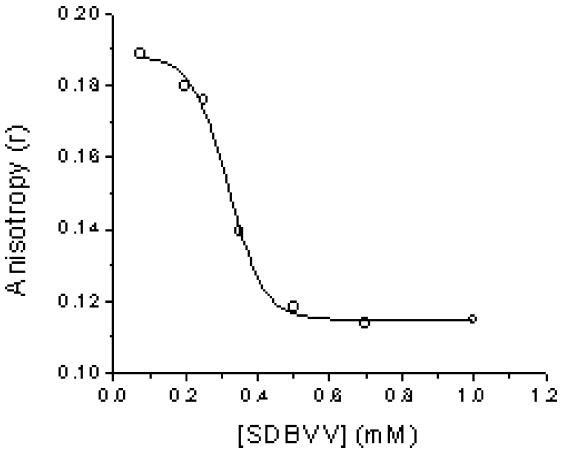

Figure 1. Plot of fluorescence anisotropy (*r*) as a function of [SDBVV].

difference in the case of SDBVA might be due to relatively large error in the measurement. However, the cac values obtained by both methods are low. A similarly low cac value was also obtained for SDBV, which has only one amino acid at the surfactant head group. The data suggest that there is no measurable difference between the cac values of the SDBVA and SDBAV. This means that the order of amino acid in the peptide head group has no significant influence on the self-assembly formation. A slightly higher cac value in the case of SDBVV may be attributed to its relatively higher hydrophobicity and the steric effect of the head group compared to that of SDBAV or SDBVA.

3.2. Fluorescence Depolarization Studies. Like the enhancement of fluorescence intensity of the NPN probe, the fluorescence anisotropy (*r*) of the DPH probe can change when bound to the hydrophobic domains of self-assemblies. In fact, fluorescence characteristics of these probes when bound to the hydrophobic domains can shed light on the nature of their microenvironments and hence the aggregate structure. In other words, the *r*-value is sensitive to a change in microstructure of the self-assemblies. We have measured fluorescence anisotropy of the DPH probe in the presence of the surfactants at a concentration above their cac value. The data are included in Table 1. The *r*-values are higher compared to SDS micelles ($r = 0.054$),[15] which suggests that the microenvironment of the probe molecule is very rigid. This is possible only if bilayer structures are formed. We have also measured the *r*-value in the presence of different concentrations of SDBVV. The variation of *r* with surfactant concentration is shown in Figure 1.

The plot clearly shows a decrease of *r* with the increase of SDBVV concentration. This may be due to transformation of vesicles to elongated micelles, which have larger sizes compared to spherical micelles. This is supported by the electron micrographs as discussed below. A similar vesicle-to-micelle transition in a *N*-acyl phenyl alaninate surfactant has also been reported recently.[16] Such studies could not be performed with the other amphiphiles because of the appearance of turbidity on standing in aqueous solutions of SDBVA and SDBAV at concentrations greater than 0.3 mM. This is perhaps due to fusion of smaller vesicles to form very large vesicles. The sigmoid plot in Figure 1 is indicative of the existence of equilibrium between vesicles and rod-like micelles. This is also suggested by the DLS and microviscosity data presented below. Chiral amino acid-derived surfactants are known to form various types of bilayer aggregates including planar bilayers, vesicles, twisted ribbons, helical strands, etc. in aqueous solution at acidic pH.[3−10] It has been suggested that at higher surfactant concentrations planar bilayer structures roll up to produce rods.[3] A similar mechanism might be also involved in the present systems.

3.3. Micropolarity and Microviscosity. As discussed above, the large blue shift of the fluorescence emission spectrum of the NPN probe suggests that the palisade layer, which is an interfacial region of the bilayer aggregates, is less polar compared to bulk water. In order to estimate the polarity of the core of the aggregates, we have employed pyrene as a fluorescent probe, which is solubilized in the hydrocarbon region of the self-assembly. The intensity ratio, I_1/I_3, of the first and the third vibronic peaks of the pyrene fluorescence spectrum is known to be sensitive to the polarity of its environment.[17] The I_1/I_3 ratio that has the highest value in water decreases with the decrease in solvent polarity. Therefore, it has been widely used as a micropolarity probe for self-assemblies.[17−20] The polarity ratio I_1/I_3 was measured in surfactant solution having concentration above cac for all the surfactants (Table 1). The value of I_1/I_3 is very low compared to that in water (1.79), which indicates that pyrene is solubilized in the hydrophobic region of the bilayer aggregates. The data suggest that SDBVV micelles have lowest micropolarity. It is interesting to note that the micropolarity (I_1/I_3 value) of pyrene is higher in SDBAV micelles than in SDBVA micelles. The values of I_1/I_3 and *r* can be correlated to the microenvironment of pyrene and DPH probes, respectively. The larger value of *r* and the smaller value of I_1/I_3 compared to the corresponding quantities in water indicate that the microenvironment of the probes is nonpolar as well as more viscous than bulk water, which is consistent with the formation of bilayer aggregates in dilute solutions. The rigidity of the microenvironments of DPH molecules is further manifested by the microviscosity (η_m) value of the self-assemblies formed. The details of microviscosity determination has been described elsewhere.[15] Briefly, η_m was calculated from the Debye−Stokes−Einstein relation:[21]

$$\eta_m = kT\tau_R/\upsilon_h \qquad (2)$$

where υ_h is the hydrodynamic volume (313 Å^3)[15] of the probe molecule and τ_R is the rotational correlation time of the fluorophore. The τ_R was calculated from Perrin's equation:[22]

$$\tau_R = \tau_f(r_o/r - 1)^{-1} \qquad (3)$$

where r_o is the steady-state fluorescence anisotropy value in a highly viscous solvent (0.362)[23] and τ_f is the fluorescence lifetime of the DPH molecule in surfactant solution. The details of time-resolved fluorescence measurements are available in the Supporting Information. The τ_f values in SDBAV (0.05 mM), SDBVA (0.05 mM), and SDBVV (0.1 mM) surfactant solutions were found to be 8.06, 6.91, and 7.51 ns, respectively. The η_m values (see Table 1) thus obtained are much higher than those of normal micelles of ionic surfactants such as SDS (16.33 mPa s).[15] The η_m values are consistent with the bilayer aggregates. It should be noted that η_m is highest in the case of SDBVV, suggesting tighter packing of the hydrocarbon chains. This may be due to similar spatial orientations of the amino acid residues in SDBVV molecule. The data in Table 1 show that at higher concentration of SDBVV the value of η_m is lower. The value is slightly higher than that of normal micelles and thus can be associated to rod-like micelles.

3.4. Transmission Electron Micrographs (TEM). In order to investigate the microstructures formed in dilute and concentrated solutions of the amphiphiles, we have measured TEM

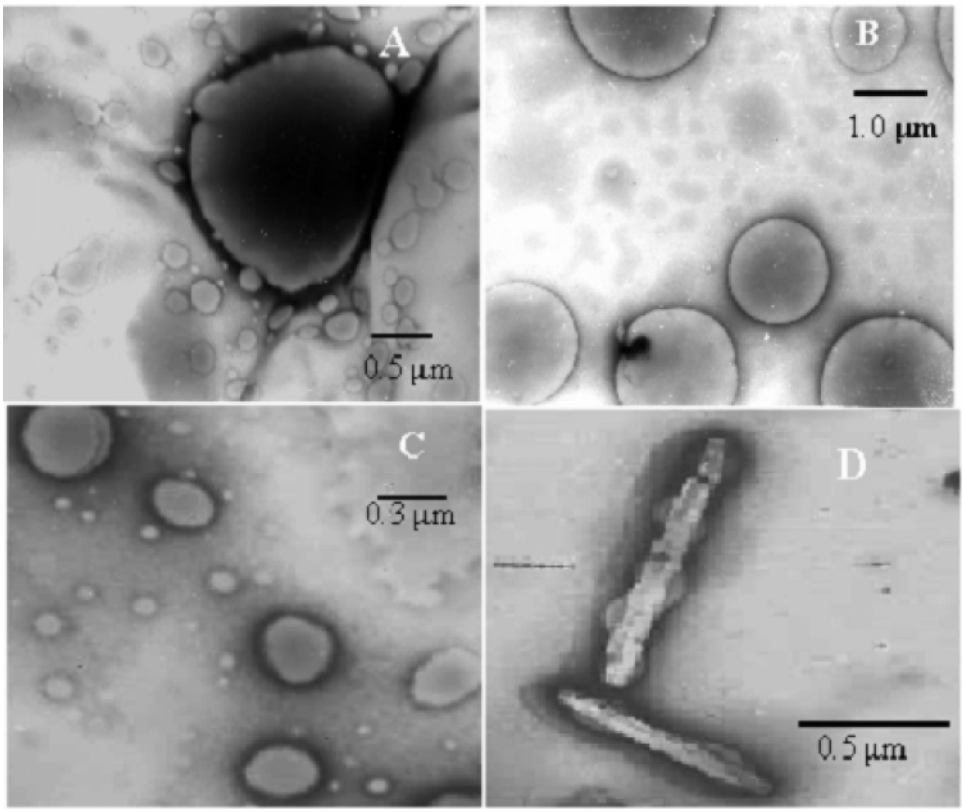

Figure 2. TEM micrographs of (A) 0.1 mM SDBVA, (B) 0.1 mM SDBAV, (C) 0.2 mM SDBVV, and (D) 6 mM SDBVV.

(Figure 2A−D). The micrographs A−C clearly exhibit large vesicular structures. The size (inner diameter) of the large vesicles ranges 100 nm to 2.5 μm. Because we were unable to measure thickness of the vesicle wall, it is difficult to confirm if they are monolayer or multilayer vesicles. The micrograph D of the concentrated (6 mM) SDBVV solution shows the presence of tubular and rod-like micelles along with the vesicle structures (not shown). Absence of any tubular or rod-like structures in dilute solutions implies that these types of aggregates are formed at higher concentrations of the amphiphiles.

3.5. Dynamic Light Scattering Studies. The DLS measurements were performed with dilute solution ($C = 5 \times$ cac) of the surfactants. For all solutions, the relaxation rate, Γ, was found to vary linearly with q^2 and the fitted lines pass through the origin (Figure 3), suggesting measurement of translational diffusion of the particles. The apparent hydrodynamic radii (R_h) calculated using the Stokes−Einstein equation are listed in Table 1. The R_h values of the aggregates formed by the amphiphiles are very large compared to that of micellar aggregates for which the typical value of R_h is typically below 5 nm.

The large size of the aggregates is consistent with the vesicular or rod-like structures. The size distribution of vesicles in all the cases was found to be monomodal, which indicates formation of only one type of aggregate. Because fluorescence depolarization studies indicate formation of bilayer aggregates, the structures are more likely to be spherical vesicles. The size of the vesicles obtained from DLS measurements is smaller than that shown by the micrographs. This might be due to filtration of solutions used for DLS measurements. Also the DLS measurement gives the average diameter of the particles. The DLS measurements performed with higher concentrations of SDBAV (0.2 mM) and SDBVV (1.0 mM) surfactants resulted in a lower R_h value. The respective values are included in Table 1. This supports our earlier conclusion derived from fluorescence depolarization studies that vesicles are transformed to smaller micellar aggregates at higher surfactant concentrations. In fact, TEM (Figure 2D) of 6 mM SDBVV solution shows the presence of rod-like aggregates.

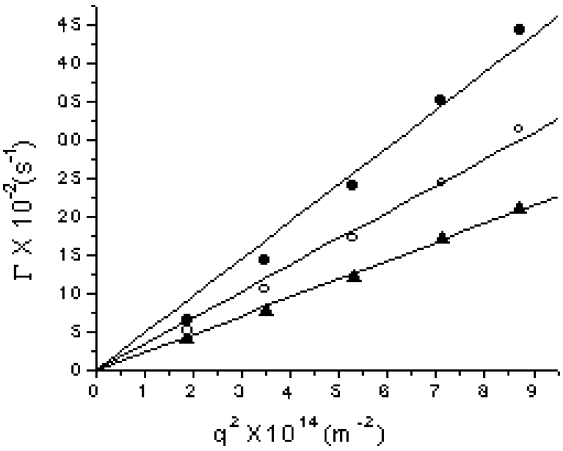

Figure 3. Plot of relaxation rate, Γ, of the self-assemblies in 0.1 mM SDBAV (●), 0.1 mM SDBVA (▲), and 0.2 mM SDBVV (○) solution as a function of the square of the scattering vector, q^2.

3.6. Circular Dichroism Spectra. In our earlier publication, we have shown that SDBV forms α-helical aggregates in dilute aqueous solution.[12] It was suggested that amide hydrogen bonding and chirality of the surfactant molecule is important for the formation of helical aggregates. In order to investigate the effect of a peptide linkage at the surfactant head group, we have measured CD spectra of SDBVA, SDBAV, and SDBVV in water at concentrations above their cac value. The spectra are presented in Figure 4. For comparison, we have also included the CD spectrum of SDBV in Figure 4. As can be seen, all the

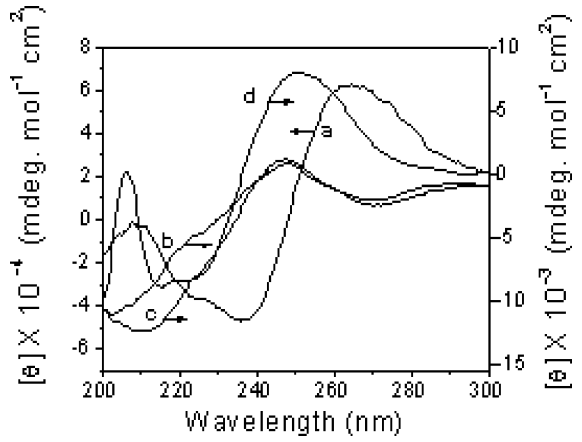

Figure 4. CD spectra of (a) 0.25 mM SDBAV, (b) 0.25 mM SDBVA, (c) 0.25 mM SDBVV, and (d) 0.125 mM SDBV in water (pH 9.1).

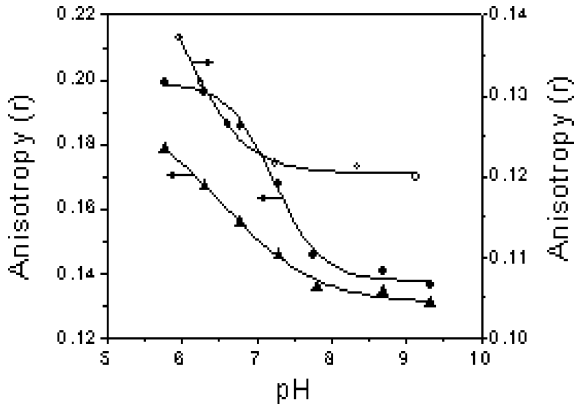

Figure 5. Effect of pH on fluorescence anisotropy (r) of DPH in 0.15 mM SDBAV (●), 0.15 mM SDBVA (▲), and 0.15 mM SDBVV (○) in water at pH 9.1.

surfactants exhibit band structure in the 220−240 nm range characteristic of helical aggregates. However, in the case of SDBAV, the molar ellipticity of the bands are much higher compared to SDBV. It is also interesting to note that the CD bands in SDBAV are red-shifted relative to that of SDBV. This may be attributed to the peptide linkage that facilitates twisting of the bilayer ribbons. However, the cause for lower ellipticity of the CD bands of SDBVA and SDBVV surfactants is not clear to us at the moment. It should be noted that no helical aggregates could be observed in the TEM micrograph of SDBAV. This might be due to the artifact of the technique, which involves drying of the sample.

3.7. pH-Dependence of Self-Organization. The fluorescence anisotropy of the DPH probe in the presence of the surfactants was monitored to study the effect of pH on the self-assembly formation. Figure 5 shows the variations of anisotropy as a function of pH for a 0.15 mM surfactant. The sigmoid change of the anisotropy value for all the three amphiphiles suggests a two-state process. This may be a result of protonation of the $-COO^-$ group that reduces ionic repulsions as well as promotes intermolecular hydrogen bonding between the $-COOH$ and $-COO^-$ or between $-COOH$ and $-CONH-$ groups at the interface. The ordering at the micellar interface should also result in compact packing in the interior of the bilayer aggregates as manifested by the increase of anisotropy with the decrease of pH. The inflection point of the plots in Figure 5 can be taken as the pK_a of the respective amphiphile. The pK_a values obtained from the inflection points are higher than the pK_a value of the

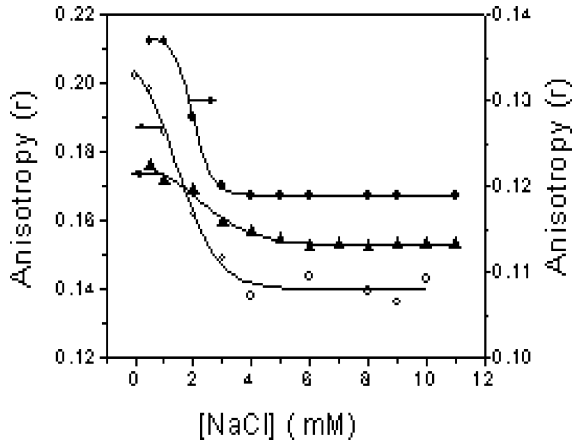

Figure 6. Effect of salt concentration on fluorescence anisotropy (r) of DPH in 0.15 mM SDBAV (●), 0.12 mM SDBVA (▲), and 0.15 mM SDBVV (○) in water (pH 9.1).

corresponding fatty acid monomers in aqueous solution (typically 5.0).[24] The increase of pK_a values may be attributed to the high charge densities on the bilayer surface. A similar increase of pK_a values has been also suggested for fatty acids by other researchers.[25−27] Thus, it can be concluded that vesicle structures are more favored at pH < 7.0. The intermolecular hydrogen bonding as a result of protonation of the $-COO^-$ group may increase the curvature of the bilayer aggregates to produce closed vesicles.

3.8. Effect of Salt Concentration. The surfactant counterion has an enormous effect on the microstructure of the self-assemblies. In order to investigate the stability of the vesicle in the presence of a salt, we have measured the fluorescence anisotropy of the DPH probe in a surfactant solution of fixed concentration containing varying concentrations of NaCl. The variation of r as a function of [NaCl] is shown in Figure 6. The plots show a decrease of r-value with the rise of salt concentration. The sigmoid nature of the plots suggests a two-state equilibrium process. This indicates transformation of ordered bilayer vesicles to some less ordered aggregates such as spherical or rod-like micelles. However, the r-value at the highest salt concentration is higher than that expected for normal micelles ($r = \sim 0.05$). Thus, formation of spherical micelles at higher salt concentration can be ruled out. Therefore, it can be concluded that the salt-induced transition is due to formation of rod-like micelles, the microenvironment of which is slightly more ordered compared to normal micelles. Although it seems counterintuitive in light of the screening of electrostatic repulsions by salt and the geometric packing consideration,[28] it is caused by a change in composition of the aggregate upon addition of salt. As discussed in the preceding section, vesicle structures are favored in acidic pH at which both carboxylate and protonated forms of the surfactants are present. The surfactants, being sodium salts of weak acids, get hydrolyzed in water according to the reaction

$$RCOO^-Na^+ + H_2O \leftrightarrow RCOOH + Na^+ + OH^- \quad (4)$$

In the presence of sodium salt, the equilibrium is shifted toward the left producing more $RCOO^-Na^+$, which at high concentrations forms rod-like micelles. Kaler and co-workers,[29] for a catanionic surfactant mixture, have also reported a salt-induced transition of vesicle to micelle.

3.9. Stability of the Vesicles. As discussed above, the initially transparent aqueous solutions of SDBAV and SDBVA surfac-

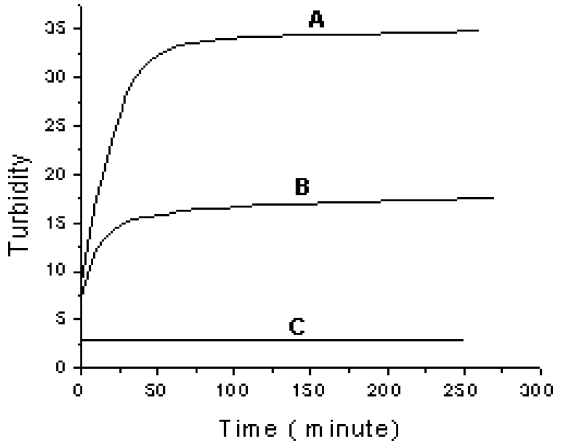

Figure 7. Time dependence of turbidity of (A) 0.6 mM SDBAV, (B) 0.6 mM SDBVA, and (C) 1.2 mM SDBVV at 30 °C.

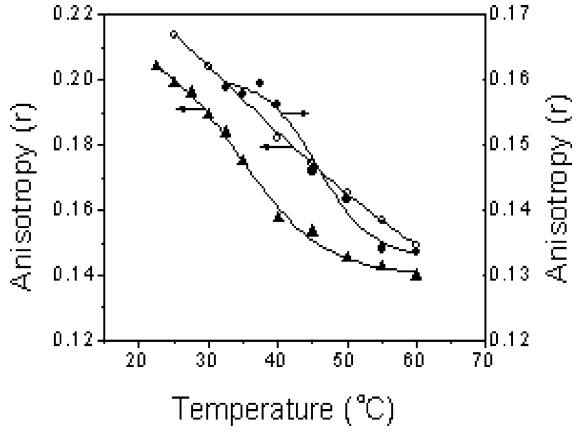

Figure 8. Variation of fluorescence anisotropy (*r*) of DPH in 0.15 mM SDBAV (●), 0.12 mM SDBVA (▲), and 0.15 mM SDBVV (○) with temperature.

tants become turbid upon standing at concentrations much higher than their cac value. The plots showing time dependence of turbidity τ (= 100 − %*T*) are shown in Figure 7. Clearly, turbidity increases with time. In the cases of SDBVA and SDBAV, an increase of concentration resulted in precipitation after 3−12 h (not shown). The SDBVV solution, however, remains transparent even after a month. The appearance of turbidity is perhaps due to association of vesicles formed by the surfactants in dilute solution. The increase of surfactant concentration enhances the rate of association of the aggregates, leading to precipitation within a short time.

3.10. Effect of Temperature. In order to study the vesicle stability against rise of temperature, we have measured the temperature variation of fluorescence anisotropy of the DPH probe solubilized in the vesicles. The plots in Figure 8 show the variation of *r* with temperature in the presence of SDBVV (0.15 mM), SDBAV (0.15 mM), and SDBVA (0.12 mM). The sigmoid plot suggests a two-state transition. Because the *r*-value is still larger at 60 °C, the decrease of *r* is perhaps due to the transition from the gel to the liquid crystalline state. The point in the sigmoid plot corresponding to a 50% change of *r* can be taken as the phase transition temperature, T_c. The data are presented in Table 1. The T_c value in all cases is ∼40 °C. This suggests that the vesicles are quite stable at body temperature (37 °C).

4. Conclusions

In summary, self-assembly formation of sodium salts of three *N*-acyl peptides was investigated. They have been shown to spontaneously form large vesicles in dilute aqueous solution. The cac values of the amphiphiles are very low, which implies that the free energy of formation of vesicles is lower. The size of the vesicles ranges 100 nm to 2.5 μm. The vesicle formation is more favored at around neutral pH. In dilute solution, the vesicle phase of the amphiphiles is quite stable. However, upon an increase of the surfactant concentration, the vesicles slowly transform into elongated (rod-like) micelles. A small increase of salt concentration also transforms vesicles to rod-like micelles, which normally is not observed with ionic surfactants. The order of the amino acid residues in the peptide linkage was found to be important for the formation of helical aggregates. Although CD spectra of all three amphiphiles suggest formation of helical aggregates, the helicity is stronger in the case of SDBAV. The effect of head group structure is also reflected in the micropolarity and microviscosity values. The microviscosity values of the vesicles formed by the three amphiphiles are much higher than that of ionic micelles. The vesicles undergo a gel to liquid crystal phase transition around 37 °C, which is close to the temperature of human body. The present study suggests that the amphiphiles may have potential uses as drug delivery vehicles in pharmaceutical industry.

Acknowledgment. This work was supported by CSIR (grant No. 05(1664)/00/EMR-II), New Delhi. DK thanks CSIR for a senior research fellowship (9/81(524)/2005-EMR-I). The authors are thankful to N. Chattopadhyay, Jadavpur University, Kolkata and P. A. Hassan, BARC, Mumbai for assistance with the fluorescence lifetime and DLS measurements, respectively.

Supporting Information Available: Synthesis, chemical identification of the amphiphiles, and details of surface tension, steady-state, and time-resolved fluorescence measurements are available. This material is available free of charge via the Internet at http://pubs.acs.org.

References and Notes

(1) Du, X.; Hlady, V. *J. Phys. Chem. B* **2002**, *106*, 7295.
(2) Zhang, Y. J.; Jin, M.; Lu, R.; Song, Y.; Jiang, L.; Zhao, Y.; Li, T. J. *J. Phys. Chem. B* **2002**, *106*, 1960.
(3) Boettcher, C.; Schade, B.; Fuhrhop, J. H. *Langmuir* **2001**, *17*, 873.
(4) Imae, T.; Takahashi, Y.; Muramatsu, H. *J. Am. Chem. Soc.* **1992**, *114*, 3414.
(5) Blanzat, M.; Massip, S.; Spéziale, V.; Perez, E.; Rico-Lattes, I. *Langmuir* **2001**, *17*, 3512.
(6) Emmanouil, V.; El Gghoul, M.; Andre-Barres, C.; Guidetti, B.; Rico-Lattes, I.; Lattes, A. *Langmuir* **1998**, *14*, 5389.
(7) Fuhrhop, J. H.; Helfrich, W. *Chem. Rev.* **1993**, 1565.
(8) Shinitzky, M.; Haimovitz, R. *J. Am. Chem. Soc.* **1993**, *115*, 12545.
(9) Du, X.; Shi, B.; Liang, Y. *Langmuir* **1998**, *14*, 3631.
(10) Köning, J.; Boettcher, C.; Winkler, H.; Zeitler, E.; Talmon, Y.; Fuhrhop, J. H. *J. Am. Chem. Soc.* **1993**, *115*, 693.
(11) Roy, S.; Dey, J. *Langmuir* **2003**, *19*, 9625.
(12) Mohanty, A.; Dey, J. *Langmuir* **2004**, *20*, 8452.
(13) Billiot, F. H.; McCarroll, M.; Billiot, E. J.; Rugutt, J. K.; Morris, K.; Warner, I. M. *Langmuir* **2002**, *18*, 2993.
(14) Saitoh, T.; Taguchi, K.; Hiraide, M. *Anal. Chim. Acta.* **2002**, *454*, 203.
(15) Roy, S.; Mohanty, A.; Dey, J. *Chem. Phys. Lett.* **2005**, *414*, 23.
(16) Ohta, A.; Tani-I, K.; Hoshiba, A.; Asakwa, T.; Miyagishi, S. *Chem. Lett.* **2005**, *34*, 560.
(17) Kalyanasundaram, K.; Thomas, J. K. *J. Am. Chem. Soc.* **1977**, *99*, 2039.
(18) Kalyansundaram, K. *Photophysics of Microheterogeneous Systems*; Academic Press: New York, 1988.
(19) Thomas, J. K. *The Chemistry of Excitation at Interfaces*; ACS Monograph 181; American Chemical Society: Washington, DC, 1984.
(20) Winnik, F. M.; Regismond, S. T. A. *Colloids Surf. A* **1996**, *118*, 1.

(21) Debye, P. *Polar Molecules*; Dover: New York, 1929.
(22) Lakowicz, J. R. *Principles of Fluorescence Spectroscopy*; Plenum Press: New York, 1983; p 132.
(23) Shinitzky, M.; Yuli, I. *Chem. Phys. Lipids* **1982**, *30*, 261.
(24) Ptak, M.; Egret-Charlier, M.; Sanson, A.; Bouloussa, O. *Biochim. Biophys. Acta* **1980**, *600*, 387.
(25) Gebicki, J. M.; Hicks, M. *Nature* **1973**, *243*, 232.
(26) Bachmann, P. A.; Luisi, P. L.; Lang, J. *Nature* **1992**, *357*, 57.
(27) Walde, P.; Wick, R.; Fresta, M.; Mangone, A.; Luisi, P. L. *J. Am. Chem. Soc.* **1994**, *116*, 11649.
(28) Israelachvili, J. N. *Intermolecular and Surface Forces*, 2nd ed.; Academic Press Inc.: San Diego, CA, 1992.
(29) Brasher, L. L.; Kaler, E. W. *Langmuir* **1996**, *12*, 6270.